

UC Irvine

UC Irvine Previously Published Works

Title

Comparative Pharmacokinetics of Δ^9 -Tetrahydrocannabinol in Adolescent and Adult Male Mice

Permalink

<https://escholarship.org/uc/item/9089q0cf>

Journal

Journal of Pharmacology and Experimental Therapeutics, 374(1)

ISSN

0022-3565

Authors

Torrens, Alexa
Vozella, Valentina
Huff, Hannah
[et al.](#)

Publication Date


2020-07-01

DOI

10.1124/jpet.120.265892

Peer reviewed

Comparative Pharmacokinetics of Δ^9 -Tetrahydrocannabinol in Adolescent and Adult Male Mice[§]

Alexa Torrens,¹ Valentina Vozella,¹ Hannah Huff, Brandon McNeil, Faizy Ahmed, Andrea Ghidini,  Stephen V. Mahler, Marilyn A. Huestis, Aditi Das, and Daniele Piomelli

Departments of Anatomy and Neurobiology (A.T., V.V., B.M., F.A., A.G., D.P.), Neurobiology and Behavior (S.V.M.), Biological Chemistry (D.P.), and Pharmaceutical Sciences (D.P.), University of California, Irvine, California; Department of Chemistry, University of Illinois at Urbana-Champaign, Urbana, Illinois (H.H., A.D.); Dipartimento di Scienza degli Alimenti e del Farmaco, Università degli Studi di Parma, Parma Italy (A.G.); and Institute of Emerging Health Professions, Thomas Jefferson University, Philadelphia, Pennsylvania (M.A.H.)

Received February 24, 2020; accepted April 27, 2020

ABSTRACT

We investigated the pharmacokinetic properties of Δ^9 -tetrahydrocannabinol (Δ^9 -THC), the main psychoactive constituent of cannabis, in adolescent and adult male mice. The drug was administered at logarithmically ascending doses (0.5, 1.6, and 5 mg/kg, i.p.) to pubertal adolescent (37-day-old) and adult (70-day-old) mice. Δ^9 -THC and its first-pass metabolites—11-hydroxy- Δ^9 -THC and 11-nor-9-carboxy- Δ^9 -THC (11-COOH-THC)—were quantified in plasma, brain, and white adipose tissue (WAT) using a validated isotope-dilution liquid chromatography/tandem mass spectrometry assay. Δ^9 -THC (5 mg/kg) reached 50% higher circulating concentration in adolescent mice than in adult mice. A similar age-dependent difference was observed in WAT. Conversely, 40%–60% lower brain concentrations and brain-to-plasma ratios for Δ^9 -THC and 50%–70% higher brain concentrations for Δ^9 -THC metabolites were measured in adolescent animals relative to adult animals. Liver microsomes from adolescent mice converted Δ^9 -THC into 11-COOH-THC twice as fast as adult microsomes. Moreover, the brains of adolescent mice contained higher mRNA levels of the multidrug transporter breast cancer resistance protein, which

may extrude Δ^9 -THC from the brain, and higher mRNA levels of claudin-5, a protein that contributes to blood-brain barrier integrity. Finally, administration of Δ^9 -THC (5 mg/kg) reduced spontaneous locomotor activity in adult, but not adolescent, animals. The results reveal the existence of multiple differences in the distribution and metabolism of Δ^9 -THC between adolescent and adult male mice, which might influence the pharmacological response to the drug.

SIGNIFICANCE STATEMENT

Animal studies suggest that adolescent exposure to Δ^9 -tetrahydrocannabinol (Δ^9 -THC), the intoxicating constituent of cannabis, causes persistent changes in brain function. These studies generally overlook the impact that age-dependent changes in the distribution and metabolism of the drug might exert on its pharmacological effects. This report provides a comparative analysis of the pharmacokinetic properties of Δ^9 -THC in adolescent and adult male mice and outlines multiple functionally significant dissimilarities in the distribution and metabolism of Δ^9 -THC between these two age groups.

Introduction

As with other psychoactive drugs, cannabis use typically starts in early teenage years and progressively increases throughout adolescence: In 2018, 35.7% of 12th graders in American schools tried the drug at least once (Johnston et al., 2019). Teenagers use cannabis more than any other recreational substance, and many also experiment with novel

synthetic cannabinoids (Johnston et al., 2019). Furthermore, the growing diffusion of medical cannabis-derived products—for example, for childhood epilepsy and autism symptoms—is exposing new groups of young people to the drug. These trends are of particular concern within a social context in which broadening acceptance and legislative changes fuel financial interests that can potentially override public health and safety concerns (Kalant, 2015; Piomelli, 2015).

Brain networks controlling human emotion and cognition are still actively developing during adolescence (Spear, 2000; Steinberg, 2005), and this plastic state makes them particularly sensitive to disruption by cannabinoid agents and other insults (Lubman et al., 2015). Indeed, there is an overall consensus across epidemiologic surveys that adolescent-onset

The study was funded by the National Institute on Drug Abuse (NIDA) [Center of Excellence Grant DA044118]. This work was supported by the National Institutes of Health [R01 GM1155884].

¹A.T. and V.V. contributed equally to this work.

<https://doi.org/10.1124/jpet.120.265892>

[§] This article has supplemental material available at jpet.aspetjournals.org.

ABBREVIATIONS: ABC, ATP-binding cassette; *Abcb1*, P-glycoprotein; *Abcg2*, breast cancer resistance protein; AUC, area under the curve; BBB, blood-brain barrier; CL, clearance; *Cldn5*, claudin-5; 11-COOH-THC, 11-nor-9-carboxy- Δ^9 -THC Ct threshold cycle; EMR, Enhanced Matrix Removal; ISTD, internal standard; LC, liquid chromatography; LC-MS/MS, LC/tandem mass spectrometry; *m/z*, mass-to-charge ratio; 11-OH-THC, 11-hydroxy- Δ^9 -THC; PCR, polymerase chain reaction; PK, pharmacokinetics; PND, postnatal day; *t*_{1/2}, half-life; Δ^9 -THC, Δ^9 -tetrahydrocannabinol; *T*_{max}, time maximum concentration reached; *V*_D, volume of distribution; WAT, white adipose tissue; λ_z , elimination rate constant.

use of cannabis is associated with impairments in cognition and affect that continue into adulthood even after use of the drug has stopped (Schweinsburg et al., 2008). Supporting a causal link between cannabis use and changes in brain function, studies showed that exposing adolescent mice and rats to the psychotropic constituent of cannabis, Δ^9 -tetrahydrocannabinol (Δ^9 -THC), or one of its synthetic mimics causes persistent dysregulations in affect, memory, and reward-seeking behavior (for review, see Rubino and Parolaro, 2016). Despite their mechanistic value, these animal experiments generally discounted the possible pharmacodynamic consequences of age-related changes in the absorption, distribution, and metabolism of Δ^9 -THC. Such changes are to be expected, however. Indeed, the scientific literature offers substantial evidence for developmental regulation of xenobiotic metabolism via the hepatic CYP₄₅₀ system (Sadler et al., 2016), plasma protein-binding activity (Sethi et al., 2016), and blood-brain barrier (BBB) function (Goodall et al., 2018). These parameters are critical to the disposition of Δ^9 -THC, a hydrophobic substance that avidly binds to serum albumin (Wahlqvist et al., 1970; Fanali et al., 2011), undergoes extensive first-pass liver metabolism (for review, see Huestis, 2007; Lucas et al., 2018) (Supplemental Fig. 1), and must enter the brain to produce its characteristic intoxicating effects.

To fill this knowledge gap, in the present study we carried out a comparative analysis of the pharmacokinetic (PK) properties of Δ^9 -THC in pubertal adolescent (37-day-old) and adult (70-day-old) male mice. We administered the drug by intraperitoneal injection, the most common route used in animal models, and quantified Δ^9 -THC and its main CYP₄₅₀ metabolites [11-hydroxy- Δ^9 -THC (11-OH-THC) and 11-nor-9-carboxy- Δ^9 -THC (11-COOH-THC)] in plasma, brain, and white adipose tissue (WAT) using an isotope-dilution liquid chromatography/tandem mass spectrometry (LC-MS/MS) assay validated following Food and Drug Administration guidelines (Vozella et al., 2019). Additionally, we measured 1) the conversion of Δ^9 -THC into 11-OH-THC and 11-COOH-THC by liver microsomal fractions; 2) the transcription in brain of multidrug transporters, P-glycoprotein (*Abcb1*) and breast cancer resistance protein (*Abcg2*), which are thought to extrude Δ^9 -THC from the brain (Leishman et al., 2018), and of claudin-5, a tight-junction protein involved in BBB integrity (Greene et al., 2019); and 3) the effects of Δ^9 -THC (5 mg/kg) on spontaneous locomotor activity. The results reveal the existence of significant dissimilarities in the distribution and metabolism of Δ^9 -THC between adolescent and adult mice, which might influence wide-ranging pharmacological responses to the drug.

Materials and Methods

Chemicals and Solvents. [²H₃]- Δ^9 -THC, [²H₃]-11-OH-THC, and [²H₃]-11-COOH-THC were purchased from Cerilliant (Round Rock, TX). Δ^9 -THC was from Cayman Chemicals (Ann Arbor, MI). All analytical solvents were of the highest grade and were obtained from Honeywell (Muskegon, MI) or Sigma-Aldrich (Saint Louis, MO). Formic acid was from Thermo Fisher (Houston, TX).

Animals. Adolescent [postnatal day (PND) at arrival: 25–30, 15–20 g] and adult (PND \geq 60, 20–25 g) male C57BL/6 mice were obtained from Charles River (Wilmington, MA). They were housed in groups of four and were allowed to acclimate for at least 3 days before experiments. Housing rooms were maintained on a 12-hour light/dark cycle (lights on at 6:30 AM) under controlled conditions of temperature

(20 \pm 2°C) and relative humidity (55%–60%). Food and water were available ad libitum. All procedures were approved (Animal Use Protocol 18-053) by the Institutional Animal Care and Use Committee at the University of California, Irvine and carried out in strict accordance with the National Institutes of Health guidelines for the care and use of experimental animals.

Pharmacokinetic Experiments. We dissolved Δ^9 -THC (Cayman) in a vehicle consisting of Tween80/saline (5:95, v/v) (Burstion et al., 2010) and administered it at ascending dosages (0.5, 1.6, or 5 mg/kg) by intraperitoneal injection to pubertal adolescent (PND 37) or adult (PND 70) mice in an injection volume of 10 ml/kg. Mice were anesthetized with isoflurane at various time points (15, 30, 60, 120, 240, and 480 minutes) after injection of one of the Δ^9 -THC doses, and blood (approximately 0.5 ml) was collected by cardiac puncture into EDTA-rinsed syringes and transferred into 1-ml polypropylene plastic tubes containing spray-coated K₂-EDTA. Plasma was prepared by centrifugation at 1450g at 4°C for 15 minutes and transferred into polypropylene tubes, which were immediately frozen and stored at –80°C. Analyses were conducted within 1 week or less of sample collection. The animals were euthanized by decapitation, and their brains were quickly removed and bisected midsagittally on an ice-cold glass plate. Epididymal WAT was collected and rinsed in cold saline. All tissue samples were frozen on dry ice and stored at –80°C until analyses.

Sample Preparation. Plasma (0.1 ml) was transferred into 8-ml glass vials (Thermo Fisher), and proteins were precipitated by addition of 0.5 ml ice-cold acetonitrile containing 1% formic acid and the following internal standards (ISTDs): [²H₃]- Δ^9 -THC, [²H₃]-11-OH-THC, and [²H₃]-11-COOH-THC, 50 pmol each. Half brains were homogenized in 5 ml ice-cold acetonitrile containing 1% formic acid. The homogenates (1 ml) were collected and spiked with 50 pmol ISTD. Epididymal WAT (20–30 mg) was homogenized in 1 ml of ice-cold acetonitrile containing 1% formic acid and 50 pmol ISTD. Plasma, brain, and WAT samples were stirred vigorously for 30 seconds and centrifuged at 2800g at 4°C for 15 minutes. After centrifugation, the supernatants were loaded onto Captiva-Enhanced Matrix Removal (EMR)-Lipid cartridges (Agilent Technologies, Santa Clara, CA) and eluted under vacuum (3–5 mm Hg). For brain and WAT fractionation, EMR cartridges were prewashed with water/acetonitrile (1:4, v/v). No pretreatment was necessary for plasma fractionation. Tissue pellets were rinsed with water/acetonitrile (1:4, v/v; 0.2 ml), stirred for 30 seconds, and centrifuged at 2800g at 4°C for 15 minutes. The supernatants were collected, transferred onto EMR cartridges, eluted, and pooled with the first eluate. The cartridges were washed again with water/acetonitrile (1:4, v/v; 0.2 ml), and vacuum pressure was increased gradually to 10 mm Hg to ensure maximal analyte recovery. Eluates were dried under N₂ and reconstituted in 0.1 ml of methanol containing 0.1% formic acid. Samples were transferred to deactivated glass inserts (0.2-ml) placed inside amber glass vials (2-ml; Agilent Technologies).

LC-MS/MS Analyses. A representative LC-MS/MS tracing is illustrated in Supplemental Fig. 2. LC separations were carried out using a 1200 series LC system (Agilent Technologies) consisting of a binary pump, degasser, thermostated autosampler, and column compartment coupled to a 6410B triple quadrupole mass spectrometric detector (Agilent Technologies). Analytes were separated on an Eclipse XDB C18 column (1.8- μ m, 3.0 \times 50.0-mm; Agilent Technologies). The mobile phase consisted of water containing 0.1% formic acid as solvent A and methanol containing 0.1% formic acid as solvent B. The flow rate was 1.0 ml/min. The gradient conditions were as follows: starting 75% B to 89% B in 3.0 minutes, this was changed to 95% B at 3.01 minutes and maintained till 4.5 minutes to remove any strongly retained materials from the column. Equilibration time was 2.5 minutes. The column temperature was maintained at 40°C and the autosampler at 9°C. The total analysis time, including re-equilibration, was 7 minutes. The injection volume was 5 μ l. To prevent carry over, the needle was washed in the autosampler port for 30 seconds before each injection using a wash solution consisting of 10% acetone in

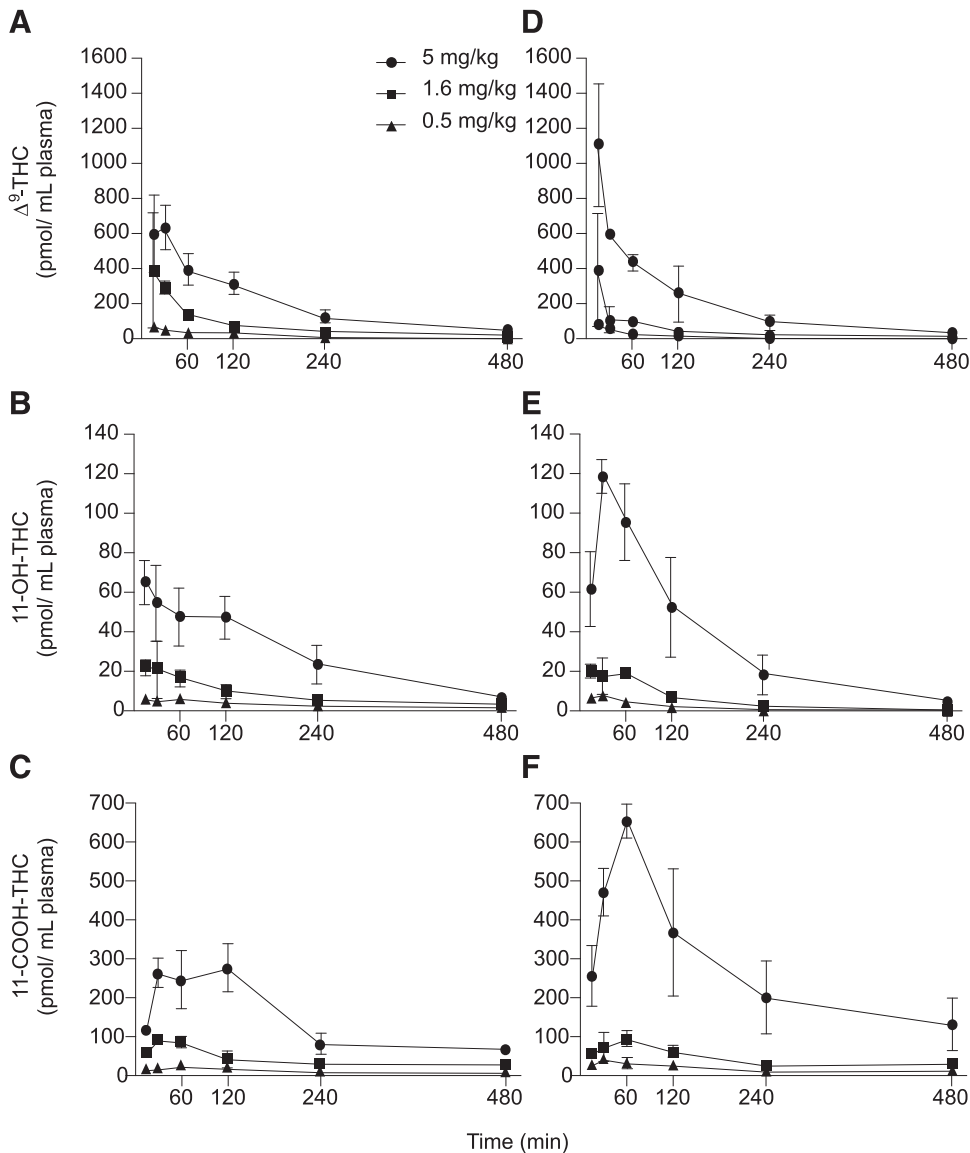


Fig. 1. Plasma concentrations of Δ^9 -THC and its first-pass metabolites, 11-OH-THC and 11-COOH-THC, after intraperitoneal injection of Δ^9 -THC (5, 1.6, 0.5 mg/kg) in adult (A–C) or adolescent (D–F) mice. Symbols represent mean \pm S.D., $n = 3$ or four animals per data point, outliers removed using Grubb's test for outliers.

water/methanol/isopropanol/acetonitrile (1:1:1:1, v/v). The MS was operated in the positive electrospray ionization mode, and analytes were quantified by multiple reaction monitoring of the following transitions: Δ^9 -THC 315.2 > 193.0 m/z , [$^2\text{H}_3$]- Δ^9 -THC 318.2 > 196.1 m/z , 11-OH-THC 331.2 > 313.1 m/z , [$^2\text{H}_3$]-11-OH-THC 334.2 > 316.1 m/z , 11-COOH-THC 345.2 > 299.2 m/z , and [$^2\text{H}_3$]-11-COOH-THC 348.2 > 302.2 m/z . In select experiments, we further verified the identity of Δ^9 -THC by monitoring the transition 315.2 > 135.0 m/z (Supplemental Fig. 2). The capillary voltage was set at 3500 V. The source temperature was 300°C, and gas flow was set at 12.0 l/min. Nebulizer pressure was set at 40 psi. Collision energy and fragmentation voltage were set for each analyte as reported (Vozella et al., 2019). The MassHunter software (Agilent Technologies) was used for instrument control, data acquisition, and data analysis.

Liver Microsome Preparation. Microsomes were prepared as described (McDougle et al., 2014) with minor modifications. Briefly, mouse livers were weighed and homogenized in extraction buffer (20%, w/v; 10 mM Tris pH 7.5, 250 mM sucrose, 1 mM phenylmethylsulfonyl fluoride, and Protease Inhibitor Cocktail, cat.: 04080-11; Nacalai Tesque, Kyoto, Japan). The homogenates were centrifuged at 3000g at 4°C for 20 minutes. Supernatants were collected and centrifuged twice for 20 minutes at 10,000g at 4°C. The supernatants

from the second centrifugation were centrifuged again for 90 minutes at 100,000g at 4°C. The microsome pellets were resuspended in 0.5-ml buffer (50 mM Tris pH 7.5, 20% glycerol, 1 mM dithiothreitol, 1 mM EDTA). Protein concentrations were measured using the bicinchoninic acid assay.

Δ^9 -THC Metabolism in Liver Microsomes. Microsomes (1 μg protein) were combined in a solution of potassium phosphate (0.1 M, pH 7.4) and rat cytochrome P_{450} reductase (0.2 μM). After a 5-minute, 37°C preincubation with Δ^9 -THC (40 μM , final concentration of DMSO was 1.2%), reactions were initiated by adding 10 mM NADPH (0.1 ml, 1 mM final) and allowed to proceed at 37°C for 30 minutes, at which point they were quenched with an equal volume of ethyl acetate. Extractions were performed as previously reported (Huff et al., 2019). Briefly, the quenched reactions were vortexed thoroughly and centrifuged for 5 minutes at 1800g at 4°C, and the organic layers were transferred into clean tubes. Fresh ethyl acetate was added, and the cycle was repeated twice for a total of three extractions. After drying down the organic layer in a rotary evaporator, extracts were resuspended in acetonitrile (0.1 ml), and 11-OH-THC and 11-COOH-THC were quantified by LC-MS/MS using a 5500 QTRAP LC-MS/MS system (Sciex, Framingham, MA) connected to a 1200 series LC system (Agilent Technologies), which included a degasser, an autosampler, and a binary

TABLE 1

C_{\max} in plasma, T_{\max} , and $t_{1/2}$ of elimination for Δ^9 -THC and its metabolites in adult and adolescent mice after intraperitoneal injection of Δ^9 -THC (5, 1.6, 0.5 mg/kg)

Data are represented as mean of $n = 4$ animals per data point. The S.E.M. was in all cases $>20\%$ and was omitted for clarity.

Analyte	Dose Δ^9 -THC (mg/kg)	Adult				Adolescent			
		C_{\max} (pmol/ml)	AUC (pmol•min/ml)	T_{\max} (min)	$t_{1/2}$ (min)	C_{\max} (pmol/ml)	AUC (pmol•min/ml)	T_{\max} (min)	$t_{1/2}$ (min)
Δ^9 -THC	5	631	91,602	30	109	1111*	86,125	15	75*
	1.6	388	32,020	15	108	392	18,080*	15	88
	0.5	71	9041	15	92	83	6261	15	89
11-OH-THC	5	65	13,050	15	123	119***	16,087	30	83**
	1.6	22	3675	15	157	21	2572	60	70***
	0.5	6	1391	60	211	8*	676**	30	86
11-COOH-THC	5	260	64,731	30	203	654***	126,607*	60	159
	1.6	94	19,977	30	253	96	20,798	60	244
	0.5	25	6104	60	225	41**	7969	30	222

* $P < 0.5$; ** $P < 0.01$; *** $P < 0.001$. Student's t test.

pump. The LC separation was performed on an Agilent Eclipse XDB-C18 column (4.6×150 -mm, 5 - μ m) with mobile phase A (0.1% formic acid in water) and mobile phase B (0.1% formic acid in acetonitrile). The flow rate was 0.4 ml/min, and the linear gradient was as follows: 0–2 minutes, 90% A; 10–23 minutes, 5% A; and 24–31 minutes, 90% A. The autosampler was set at 5°C , and the injection volume was 10 μ l. Mass spectra were acquired under positive (ion spray voltage 5500 V) electrospray ionization. The source temperature was 450°C . The curtain gas, ion source gas 1, and ion source gas 2 were 32, 65, and 50 psi, respectively. Multiple reaction monitoring was used for quantitation: Δ^9 -THC $315.2 > 193.0$ m/z ; 11-OH-THC $331.2 > 331.2$ m/z ; and 11-COOH-THC $345.2 > 327.2$ m/z . Internal standard was [$^2\text{H}_9$]- Δ^9 -THC ($324.2 > 202.1$ m/z). Software Analyst 1.6.2 was used for data acquisition and analysis.

Reverse-Transcription Polymerase Chain Reaction Analyses. Total RNA was prepared from brain tissue of adolescent (PND 37) and adult (PND 70) male mice using an Ambion PureLink RNA minikit (Life Technologies, Carlsbad, CA) as directed by the supplier. Samples were treated with DNase (PureLink DNase; Life Technologies), and cDNA synthesis was carried out using Applied Biosystems High Capacity cDNA Reverse Transcription Kit (ThermoFisher) according to the manufacturer's protocol using purified RNA (2 μ g). First-strand cDNA was amplified using the QuantiFast SYBR Green PCR Kit (Qiagen, Hilden, Germany), fluorogenic probes, and oligonucleotide primers. Copy numbers of cDNA targets were quantified at the point during cycling when the PCR product was first detected. Gene-specific primers for mouse ATP-binding cassette (ABC) transporters, *Abcb1* (F: 5'-CCCGGCTCACAGATGATGTT-3' and R: 5'-TTC CAGCCACGGGTAAATCC-3') and *Abcg2* (F: 5'-CAGCAAGGAAAG ATCCAAAGGG-3' and R: 5'-CACAAACGTCATCTTGAACCACA-3'), and integral membrane protein, claudin-5 (*Cldn5*) (F: 5'-TGACTG CCTTCCTGGACCACAA-3' and R: 5'-CATACACCTTGCACTGCA TGTGC-3'), were purchased from Life Technologies. Quantitative PCR was performed in 96-well PCR plates and run at 95°C for 10 minutes, which was followed by 40 cycles, with each cycle consisting of 15 seconds at 95°C and 1 minute at 60°C , using a Stratagene Mx 3000P (Agilent). The BestKeeper software (Pfaffl et al., 2004) was used to determine expression stability and geometric mean of different housekeeping genes (*glyceraldehyde-3-phosphate dehydrogenase* and *Actin-b*). Change in threshold cycle (Ct) values were calculated by subtracting the Ct value of the geometric mean of these housekeeping genes from the Ct value for the genes of interest. The relative quantity of the genes of interest was calculated by the expression $2^{-\Delta\Delta\text{Ct}}$. Results are reported as fold induction over control.

Motor Activity. Animals were habituated to the test cages for 3 days prior to trial. Adult and adolescent mice were injected intraperitoneally with vehicle (Tween80/saline, 5:95, v/v) or Δ^9 -THC (5 mg/kg), and motor activity was recorded using an automated system (TSE Technical & Scientific Equipment GmbH, Bad Homburg,

Germany) starting at 9:00 AM and lasting for 6 hours; the first 2 hours of activity were analyzed. The system consisted of cages equipped with an activity-detecting frame with 6×2 infrared sensors in the XY-plane (56 mm apart on the long axis, 140 mm apart on the short) and four sensors in the Z plane (56 mm apart). The XY plane, the recorded horizontal position of the animal, and the Z plane detected rearing and jumps (vertical activity). Each sensor consisted of a transmitting and receiving component arranged at right angles. Sensors scanned sequentially at a rate of 56 Hz to determine the coordinates of each animal. Each sensor interruption was registered as a "beam break." The data were analyzed as average number of beam breaks per 30 minutes.

Analyses of PK Data. We analyzed PK data using a noncompartmental model (Gabrielsson and Weiner, 2012). C_{\max} and area under the curve (AUC) were measured using GraphPad Prism 8 (La Jolla, CA) and other PK parameters [elimination rate constant (λ_z), clearance (CL), volume of distribution (V_D), and half-life ($t_{1/2}$) time of elimination] were determined as described (Gabrielsson and Weiner, 2012). In regard to CL and V_D calculations, the following equations were used: $\text{CL} = \text{dose}/\text{AUC}$; $V_D = \text{CL}/\lambda_z$. Times maximum concentrations reached (T_{\max}) were determined by visual inspection of averaged data.

Statistical Analyses. Data were analyzed using GraphPad Prism 8 by either Student's unpaired t test or two-way ANOVA with Bonferroni post hoc analysis. Outliers were determined using Grubbs' outlier test. Differences between groups were considered statistically significant at $P < 0.05$.

Results

Pharmacokinetic Profile of Δ^9 -THC in Mouse Plasma. Figure 1, A–C shows the plasma PK profiles for Δ^9 -THC and its two main first-pass metabolites, 11-OH-THC and 11-COOH-THC, in adult (PND 70) male mice after intraperitoneal administration of logarithmically ascending doses of Δ^9 -THC (0.5, 1.6, or 5 mg/kg). Table 1 reports the C_{\max} in plasma, the AUC, T_{\max} , and the half-life ($t_{1/2}$) time of elimination for each of the three compounds. At the 5 mg/kg dose, Δ^9 -THC reached a C_{\max} of 631 ± 64 pmol/ml (198 ± 20 ng/ml, mean \pm S.E.M.) with a T_{\max} of 30 minutes. Maximal plasma concentrations of 11-OH-THC and 11-COOH-THC were 65 ± 6 pmol/ml and 260 ± 18 pmol/ml, respectively, and were also reached 30 minutes after injection. Plasma $t_{1/2}$ values for Δ^9 -THC were comparable across dosages (109 ± 7 minutes at 5 mg/kg, 108 ± 18 minutes at 1.6 mg/kg, and 92 ± 10 minutes at 0.5 mg/kg). The apparent V_D of Δ^9 -THC in

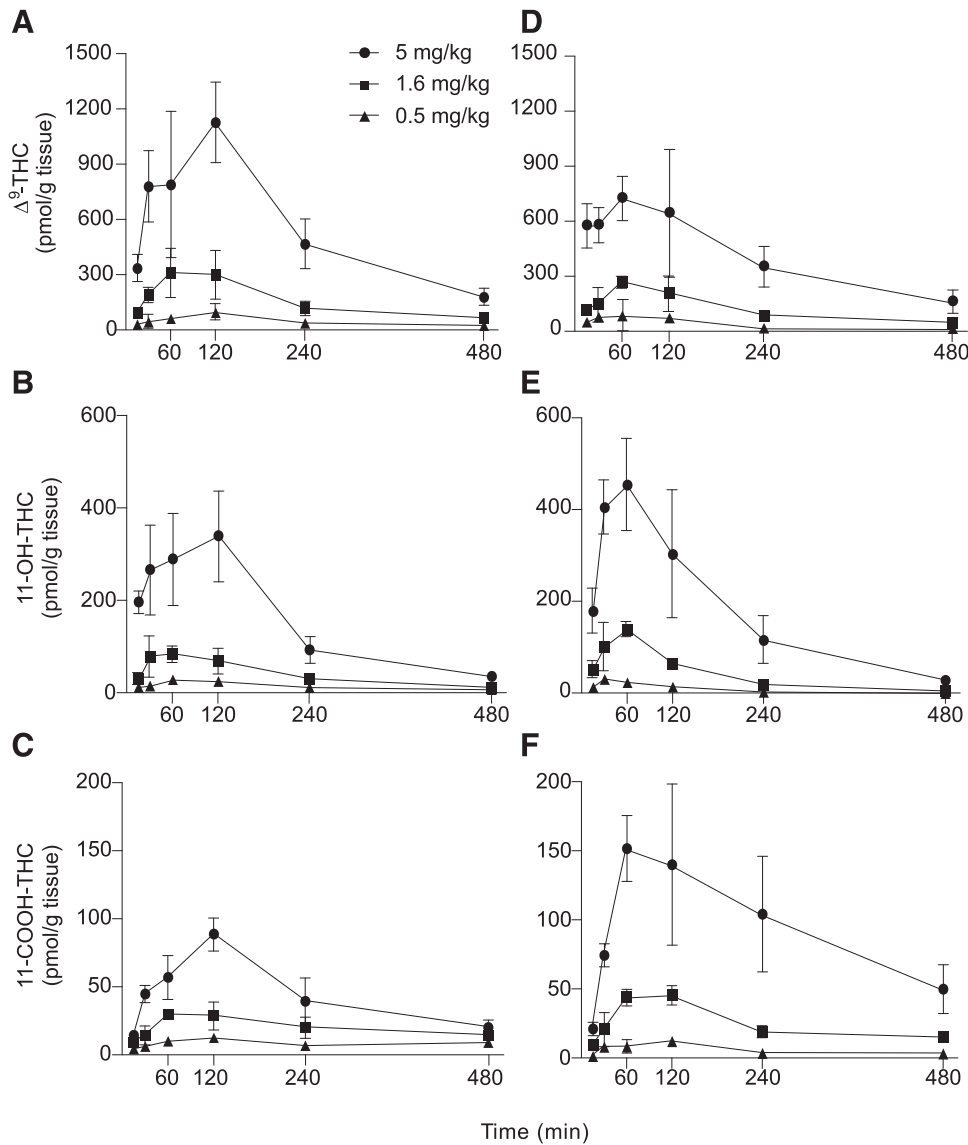


Fig. 2. Brain concentrations of Δ^9 -THC, 11-OH-THC, and 11-COOH-THC after intraperitoneal injection of Δ^9 -THC (5, 1.6, 0.5 mg/kg) in adult (A–C) or adolescent (D–F) mice. Symbols represent mean \pm S.D., $n = 3$ or four animals per data point, outliers removed using Grubb's test for outliers.

adult mice, calculated using a noncompartmental pharmacokinetic model (Gabrielsson and Weiner, 2012), was 808 ± 83 ml ($\lambda_z = 0.005 \pm 0.0004$), and CL was 4.4 ± 0.2 ml/min.

Similar plasma PK profiles were observed in pubertal adolescent (PND 37) mice, with some notable exceptions (Fig. 1, D–F; Table 1). At the 5 mg/kg dose, the C_{max} for Δ^9 -THC was 76% higher in adolescents than in adults. Moreover, at the 5- and 0.5-mg/kg doses, plasma C_{max} and AUC values for Δ^9 -THC metabolites were greater than the corresponding concentrations in adult mice. For example, after injection of 5 mg/kg Δ^9 -THC, the C_{max} for 11-COOH-THC was 2.5 times higher in adolescents than in adults (654 ± 22 vs. 260 ± 18 pmol/ml). At the same dose, the plasma T_{max} for Δ^9 -THC occurred earlier in adolescent animals (15 minutes) than in adult animals (30 minutes), and elimination was faster ($t_{1/2} = 75 \pm 9$ vs. 109 ± 7 minutes). The V_D of Δ^9 -THC in adolescents was 442 ± 54 ml ($\lambda_z = 0.008 \pm 0.001$), and the CL was 3.6 ± 0.1 ml/min, and both were lower ($P < 0.05$) than the corresponding values in adults, providing a possible explanation for the higher peak concentrations of Δ^9 -THC in plasma compared with adults.

Pharmacokinetic Profile of Δ^9 -THC in Brain. The PK profiles of Δ^9 -THC and its metabolites in the brain of adult mice are illustrated in Fig. 2, A–C. Key PK parameters are reported in Table 2. At 5 mg/kg, the C_{max} for Δ^9 -THC was 1126 ± 110 pmol/g, the T_{max} was 120 minutes, and the $t_{1/2}$ of elimination was 119 ± 9 minutes. Notably, the brain-to-plasma ratio of Δ^9 -THC was relatively low (1.9 ± 0.4) (Table 3) but consistent with values previously reported in the literature (Watanabe et al., 1980; Spiro et al., 2012). 11-OH-THC and 11-COOH-THC reached C_{max} values of 339 ± 49 and 89 ± 6 pmol/g, respectively, both at a T_{max} of 120 minutes (Table 2). The brain-to-plasma ratios for 11-OH-THC and 11-COOH-THC were 6.4 ± 0.9 and 0.4 ± 0.04 , respectively (Table 3).

Comparing the data in Fig. 2, A and D shows that at the 5-mg/kg dose, brain C_{max} for Δ^9 -THC was 55% higher in adult than in adolescent mice. The AUC was also 38% higher in the older group (Table 2). Conversely, C_{max} and AUC values for Δ^9 -THC metabolites were either lower or showed trends to be lower in adult animals. Lastly, the brain-to-plasma ratios for

TABLE 2

C_{\max} in brain, T_{\max} , and $t_{1/2}$ of elimination for Δ^9 -THC and its metabolites in adult and adolescent mice after intraperitoneal injection of Δ^9 -THC (5, 1.6, 0.5 mg/kg)

Data are represented as mean of $n = 4$ animals per data point. The S.E.M. was in all cases $>20\%$ and was omitted for clarity.

Analyte	Dose Δ^9 -THC (mg/kg)	Adult				Adolescent			
		C_{\max} (pmol/g)	AUC (pmol•min/g)	T_{\max} (min)	$t_{1/2}$ (min)	C_{\max} (pmol/g)	AUC (pmol•min/g)	T_{\max} (min)	$t_{1/2}$ (min)
Δ^9 -THC	5	1126	261,854	120	119	725*	190,080	60	134
	1.6	309	75,169	60	182	271	56,280	60	145
	0.5	97	23,044	120	155	85	16,693	60	149
11-OH-THC	5	339	71,942	120	97	454	82,399	60	93
	1.6	83	18,582	60	129	140**	19,758	60	86**
	0.5	28	6437	60	162	33	4272	30	85*
11-COOH-THC	5	89	21,240	120	147	151**	45,864*	60	239
	1.6	29	9688	120	284	46*	11,946	120	209
	0.5	13	4067	120	296	12	2781	120	198

* $P < 0.5$; ** $P < 0.01$; *** $P < 0.001$. Student's t test.

Δ^9 -THC and its metabolites were higher in adults than in adolescents (Table 3). In sum, the findings suggest that adolescent mice treated with Δ^9 -THC attain lower peak brain concentrations of the nonmetabolized drug but higher brain concentrations of its metabolites relative to adults. This finding is suggestive of age-dependent changes in the ability of Δ^9 -THC and its metabolites to access the brain and raises the intriguing possibility that the drug might undergo local metabolism within the central nervous system.

Pharmacokinetic Profile of Δ^9 -THC in WAT. Figure 3 shows the PK profiles of Δ^9 -THC and its first-pass metabolites in epididymal WAT. PK parameters are reported in Table 4. In adult mice, injection of 5 mg/kg Δ^9 -THC produced a C_{\max} of 134 ± 16 nmol/g (1.34×10^5 pmol/g) at a T_{\max} of 30 minutes (Fig. 3A). The C_{\max} for 11-OH-THC was 2 ± 0.2 nmol/g (at T_{\max} 30 minutes) and the C_{\max} for 11-COOH-THC was 0.1 ± 0.01 nmol/g (at T_{\max} 120 minutes) (Fig. 3, B and C). Because Δ^9 -THC concentrations in WAT remained virtually unchanged for the entire duration of the experiment (8 hours), $t_{1/2}$ values could not be calculated. The WAT-to-plasma ratio for Δ^9 -THC was 200.9 ± 7.9 , more than 100 times higher than the brain-to-plasma ratio, whereas the corresponding values for 11-OH-THC and 11-COOH-THC were 29.7 ± 3.8 and 0.4 ± 0.02 , respectively (Table 3), a striking confirmation that adipose tissue serves as a depot for Δ^9 -THC and its metabolites (Kreuz and Axelrod, 1973).

In WAT of adolescent mice, C_{\max} and AUC values for Δ^9 -THC were 81% and 61% higher, respectively, than in adults at the 5 mg/kg dose. The C_{\max} for 11-COOH-THC was greater in adolescents than in adults at 5 mg/kg, whereas no statistically detectable differences were seen with 11-COOH-THC at lower Δ^9 -THC doses or with 11-OH-THC at any Δ^9 -THC dose. Inconsistent variations were observed in T_{\max} , which, depending on dose and analyte, could be higher, lower, or unchanged between the two age groups (Table 4). Notably, the WAT-to-plasma ratio for Δ^9 -THC was comparable in younger and older animals, whereas lower ratios were seen in the former group for both 11-OH-THC and 11-COOH-THC (Table 3). Overall, the results are indicative of a more pronounced accumulation of Δ^9 -THC per unit weight of WAT in adolescent mice compared with adults.

Δ^9 -THC Metabolism in Liver Microsomes. The different plasma profiles of 11-COOH-THC in adolescent and adult mice raise the possibility that Δ^9 -THC may undergo age-related changes in first-pass metabolism (Fig. 1; Table 1). To

test this, we measured the sequential transformation of Δ^9 -THC into 11-OH-THC and 11-COOH-THC (Supplemental Fig. 1) by liver microsomes. In microsomal preparations from adolescent mice, Δ^9 -THC was converted into 11-COOH-THC at a rate of 0.012 ± 0.003 pmol/min per milligram, which was approximately twice as rapid as the rate measured in adult microsomes (0.006 ± 0.002 pmol/min per milligram) (Fig. 4A). By contrast, the biotransformation of Δ^9 -THC into 11-OH-THC was somewhat slower in adolescents compared with adults (adolescents: 1.5 ± 0.19 pmol/min per milligram; adults: 1.9 ± 0.05 pmol/min per milligram) (Fig. 4B). These findings are consistent with the hypothesis that adolescent mice metabolize Δ^9 -THC into 11-COOH-THC more effectively than adults do.

ABC Transporter and Claudin-5 mRNA Levels in Brain. The brain-to-plasma ratio for Δ^9 -THC was lower in adolescent mice (Table 3), suggesting that the ability of the drug to access the brain may change with age. To begin testing this hypothesis, we quantified mRNA levels of *Abcg2* and *Abcb1*, two ABC transporters present that are thought to extrude Δ^9 -THC across the BBB (Spiro et al., 2012). Extracts of adolescent brain tissue contained $P < 0.5$ higher levels of *Abcg2* transcript compared with adult tissue (Fig. 5A). By contrast, *Abcb1* mRNA levels were similar in the two age groups (Fig. 5B). We also measured transcription of *Cldn5*, a tight junction protein that contributes to BBB structure (Nitta et al., 2003), and found that its mRNA levels were $P < 0.5$ higher in adolescent brains than in adult brains (Fig. 5C). Thus, alterations in the expression of structural and functional constituents of the BBB might account for the lower Δ^9 -THC concentrations observed in the brains of adolescent mice.

TABLE 3

Tissue-to-plasma ratio for Δ^9 -THC and its metabolites (11-OH-THC and 11-COOH-THC) in brain or WAT from adolescent and adult mice after intraperitoneal injection of Δ^9 -THC (5 mg/kg)

Analyte	Dose Δ^9 -THC	Brain:Plasma		WAT:Plasma	
		Adult	Adolescent	Adult	Adolescent
Δ^9 -THC	5 mg/kg	1.9	0.8*	200.9	242.5
11-OH-THC		6.3	3.8*	29.7	19.6*
11-COOH-THC		0.4	0.2**	0.4	0.2***

* $P < 0.5$; ** $P < 0.01$; *** $P < 0.001$. Student's t test, $n = 4$ animals per data point.

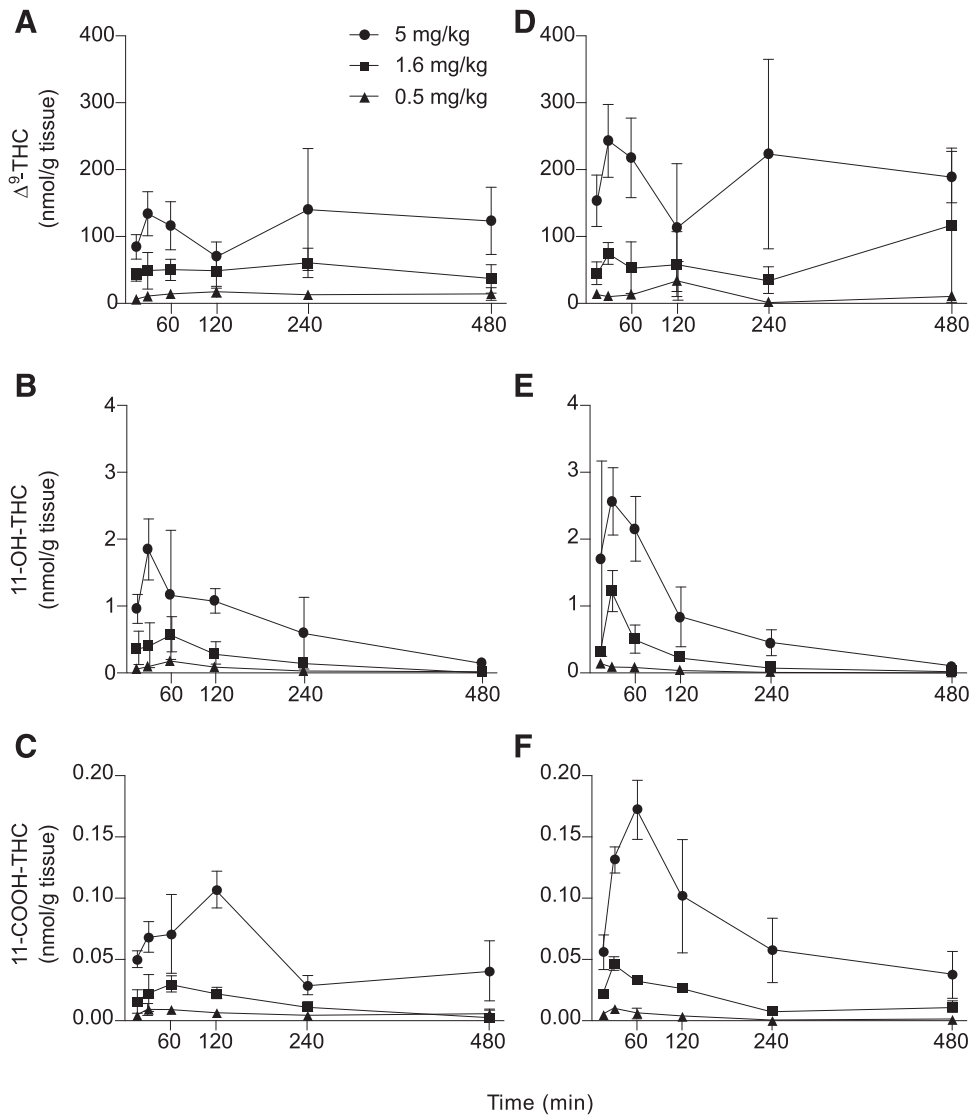


Fig. 3. WAT concentrations of Δ^9 -THC, 11-OH-THC, and 11-COOH-THC after intraperitoneal injection of Δ^9 -THC (5, 1.6, 0.5 mg/kg) in adult (A–C) or adolescent (D–F) mice. Symbols represent mean \pm S.D., $n = 3$ or four animals per data point, outliers removed using Grubb's test for outliers.

Motor Effects of Δ^9 -THC in Adolescent and Adult Mice. A comparative pharmacodynamic evaluation of adolescent versus adult mice is beyond the scope of the present study. However, a testable prediction from the PK data presented above is that adolescents might be less sensitive than adults to the effects of Δ^9 -THC. To test this, we administered vehicle (saline, 0.9%) or Δ^9 -THC (5 mg/kg) to groups of adolescent and adult male mice ($n = 10$ per group) and measured locomotor activity in a familiar environment for the following 2 hours. The results, illustrated in Fig. 6, suggest that Δ^9 -THC caused a rapid and short-lived decrease in locomotor activity in adult, but not adolescent, male mice. This finding supports the possibility suggested by our PK studies that the central nervous system of adolescent mice is partially protected from the pharmacological effects of Δ^9 -THC.

Discussion

The long-term consequences of Δ^9 -THC exposure during adolescence have been the object of many animal studies (for

a recent review, see Rubino and Parolaro, 2016), but the question of whether the PK properties of the drug might change in the transition from adolescence to adulthood was not systematically addressed. Filling this gap is important, however, to understand whether age-dependent changes in the pharmacological response to Δ^9 -THC may result solely from developmental alterations in endocannabinoid signaling—for example, in the number of cannabinoid receptors or intrinsic activity of the endocannabinoid system—or might also involve adjustments in the distribution, biotransformation, and elimination of the drug. In the present report, we assessed the PK behavior of Δ^9 -THC and its two primary first-pass metabolites, 11-OH-THC and 11-COOH-THC, following intraperitoneal administration in adolescent and adult male mice. The results identify multiple dissimilarities in the distribution and metabolism of Δ^9 -THC between the two age groups, including potentially relevant differences in peak drug concentrations in plasma and brain, brain-to-plasma ratio, and CYP₄₅₀-mediated metabolism. These results may have wide-ranging implications for the interpretation of mouse adolescent Δ^9 -THC exposure studies.

TABLE 4

C_{\max} in WAT, T_{\max} , and $t_{1/2}$ of elimination for Δ^9 -THC and its metabolites in adult and adolescent male mice after intraperitoneal injection of Δ^9 -THC (5, 1.6, 0.5 mg/kg)

Data are represented as mean of $n = 4$ animals per data point. The S.E.M. was in all cases $>20\%$ and was omitted for clarity.

Analyte	Dose Δ^9 -THC (mg/kg)	Adult			Adolescent		
		C_{\max} (nmol/g)	AUC (nmol•min/g)	T_{\max} (min)	C_{\max} (nmol/g)	AUC (nmol•min/g)	T_{\max} (min)
Δ^9 -THC	5	134	55,291	30	242*	89,246	30
	1.6	51	23,509	60	75	29,904	30
	0.5	18	6677	120	34	5863	120
11-OH-THC	5	2	323	30	3	336	30
	1.6	0.6	91	60	1*	93	30
	0.5	0.2	25	60	0.1	14*	15
11-COOH-THC	5	0.1	25	120	0.2**	35	60
	1.6	0.03	6	60	0.05*	8	30
	0.5	0.01	3	60	0.01	1*	30

* $P < 0.5$; ** $P < 0.01$; *** $P < 0.001$. Student's t test.

In the present report, we selected the intraperitoneal route of administration for two reasons: first, it is the route most frequently used in animal studies, and second, it represents a realistic compromise between experimental feasibility and human relevance. In fact, our results show that intraperitoneal injection results in substantial and reproducible tissue concentrations of Δ^9 -THC in both adolescent and adult mice and produces peaks in plasma concentrations that are quantitatively comparable to those observed in adult nonmedical cannabis smokers (Huestis, 2007). For example, the data reported in Table 1 show that the C_{\max} for Δ^9 -THC after administration of a 5-mg/kg dose in adult mice (198 ± 20 ng/ml at 30 minutes) is similar to the C_{\max} measured in the blood of persons who smoked one cannabis cigarette containing ~ 34 mg of Δ^9 -THC (162 ± 34 ng/ml at ~ 8 minutes) (Huestis and Cone, 2004). Such exposure levels are known to be associated with psychotropic activity in humans (Huestis and Cone, 2004; Cooper and Haney, 2009) as well as in rodents (Pertwee, 2008) and, in the present study, yielded micromolar concentrations of Δ^9 -THC in the brain (1126 ± 110 pmol/g, ~ 1.1 μ M), which are likely to fully engage cannabinoid receptors (Pertwee, 2008).

At the 5-mg/kg dose, the peak plasma concentrations (C_{\max}) of Δ^9 -THC, 11-OH-THC and 11-COOH-THC were all substantially greater in adolescent than in adult mice (Table 1): Δ^9 -THC C_{\max} was 76% higher, 11-OH-THC was 83% higher, and 11-COOH-THC was 152% higher. The AUC for 11-COOH-THC was almost twice as large in adolescents as it was in adults (Table 1). Higher C_{\max} and AUC values may be consequent to a weaker diversion toward WAT, whose total mass rises as mice become adults, as also suggested by the lower V_D measured in the adolescent group. Irrespective of its origin, greater Δ^9 -THC availability might account for the higher 11-OH-THC and 11-COOH-THC concentrations measured in adolescent plasma. Two findings suggest, however, that accrued metabolism might also contribute. First, adolescents eliminated Δ^9 -THC at a faster rate than adults did: The plasma $t_{1/2}$ was shorter in the younger group. Second, experiments with liver microsomes—in which the majority of Δ^9 -THC biotransformation is thought to occur (Christensen et al., 1971; Agurell et al., 1986; Watanabe et al., 1993)—show that the conversion of Δ^9 -THC into the inactive metabolite 11-COOH-THC was faster in adolescents (Fig. 5), a result consistent with the known trajectory of CYP₄₅₀ expression in the developing liver (Sadler et al., 2016).

Since plasma concentrations of Δ^9 -THC were higher in adolescent mice than in adult mice, we expected to find a parallel dissimilarity in the brain. This prediction turned out to be incorrect. In fact, C_{\max} , AUC, and brain-to-plasma ratio for Δ^9 -THC (5 mg/kg) were substantially lower in adolescent animals (Tables 2 and 3). The brain-to-plasma ratio for Δ^9 -THC was 1.9 ± 0.4 in adults, which is consistent with values reported in the literature (Watanabe et al., 1980; Spiro et al., 2012), but only 0.8 ± 0.1 in adolescents. Similarly, the brain C_{\max} for Δ^9 -THC was 1126 ± 110 pmol/g in adults and 725 ± 60 pmol/g in adolescents. Supporting these results, pharmacological experiments showed that Δ^9 -THC (5 mg/kg) lowered spontaneous locomotor activity in adult, but not adolescent, mice (Fig. 6). These findings raised the possibility that mechanisms might exist in adolescents that limit the entry of Δ^9 -THC into the central nervous system. As an initial test of this idea, we quantified mRNA levels of two multidrug ABC transporters, *Abcb1* and *Abcg2*, which were implicated in the removal of Δ^9 -THC from brain parenchyma (Spiro et al., 2012). We found that the transcription of *Abcg2*, but not *Abcb1*, was significantly higher in adolescent compared with adult mice (Fig. 5). A similar difference was seen with claudin-5, a protein that is involved in gap junction structure and BBB function (Nitta et al., 2003) and is downregulated in adult mice after a single administration of Δ^9 -THC (3 mg/kg, i.p.)

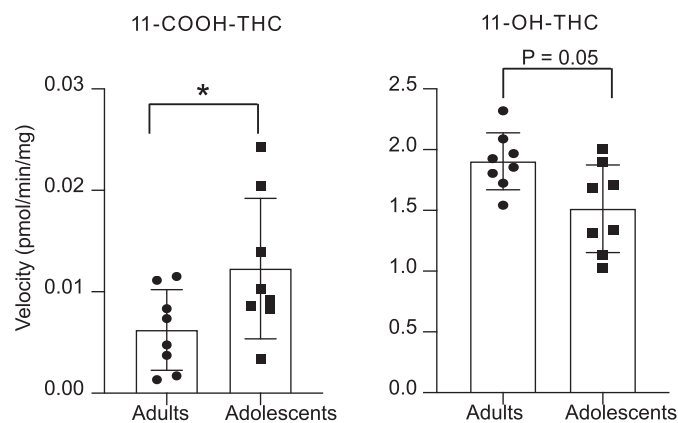


Fig. 4. Rate of formation (picomoles per minute per milligram) of 11-COOH-THC (left) and 11-OH-THC (right) in liver microsomes of adult (●) and adolescent (■) mice. Bars represent mean \pm S.D., $P < 0.05$, $n = 4$ animals per data point, Student's t test.

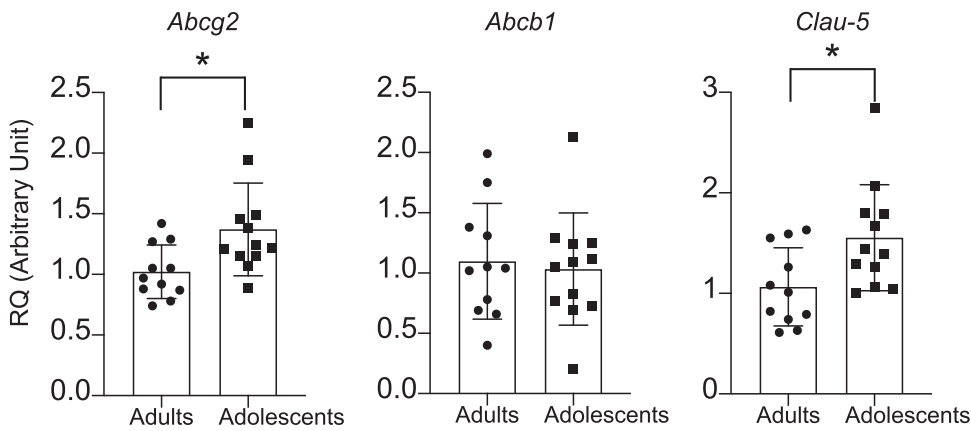


Fig. 5. mRNA levels (RQ, Arbitrary Units) of ABC transporters, *Abcg2* (left), *Abcb1* (center), and *Cldn-5* (right) in brain of adult (●) and adolescent (■) mice. Bars represent mean \pm S.D., $P < 0.05$, $n = 11$ or 12 animals per data point, Student's t test.

(Leishman et al., 2018). Thus, developmental alterations in *Abcg2* and *Cldn5* transcription and associated changes in blood/brain transfer function might contribute to the differences in brain Δ^9 -THC concentration and pharmacodynamic response observed between adolescent and adult mice. Even though the brain access of Δ^9 -THC is detectably lower in adolescent mice than adult mice, the concentrations of Δ^9 -THC metabolites in the brain showed an opposite trend. For example, at the 1.58- and 5-mg/kg doses of Δ^9 -THC, 11-COOH-THC levels were 40%–70% higher in adolescents than in adults. Potential explanations for this intriguing finding might be the existence of age-dependent changes in either the transport of Δ^9 -THC metabolites across the BBB and/or the metabolism of Δ^9 -THC in brain tissue. These explanations are nonexclusive, and testing them will require additional experimentation.

The role of WAT as a reservoir for Δ^9 -THC is well-established in the literature (Kreuz and Axelrod, 1973; Rawitch et al., 1979; Johansson et al., 1989). Adipose cells can store this hydrophobic substance for weeks after a single injection (Kreuz and Axelrod, 1973) and can release it into the bloodstream when stimulated by lipolytic signals, such as fasting or exercise (Gunasekaran et al., 2009; Wong et al.,

2013). Consistent with those data, we found that Δ^9 -THC (5 mg/kg) reached submillimolar concentrations in WAT and that such levels remained virtually unchanged for the following 8 hours (Fig. 4). Notably, the PK profile for Δ^9 -THC (5 mg/kg) in WAT displayed a unique bimodal shape that distinguished it from plasma and brain (Fig. 4). This might be due to the close anatomic proximity between injection sites in the peritoneum and epididymal fat depots. It is possible but remains to be demonstrated that the first peak results from the direct diffusion of Δ^9 -THC from the peritoneal cavity into WAT, whereas the second occurs after the drug has entered the bloodstream. We noted several additional differences between adolescent and adult animals in the PK behavior of Δ^9 -THC in WAT. For example, depending upon the dose, T_{max} could be longer, earlier, or unchanged across age groups (Table 4). Despite these discrepancies, wherein interpretation is unclear, the overall results are indicative of a greater accumulation of Δ^9 -THC and its metabolites per unit weight of adolescent WAT.

The present report has several limitations, two of which are especially noteworthy. First, our experiments were restricted to male animals and did not address possible sexual dimorphisms in the PK properties of Δ^9 -THC. Previous research

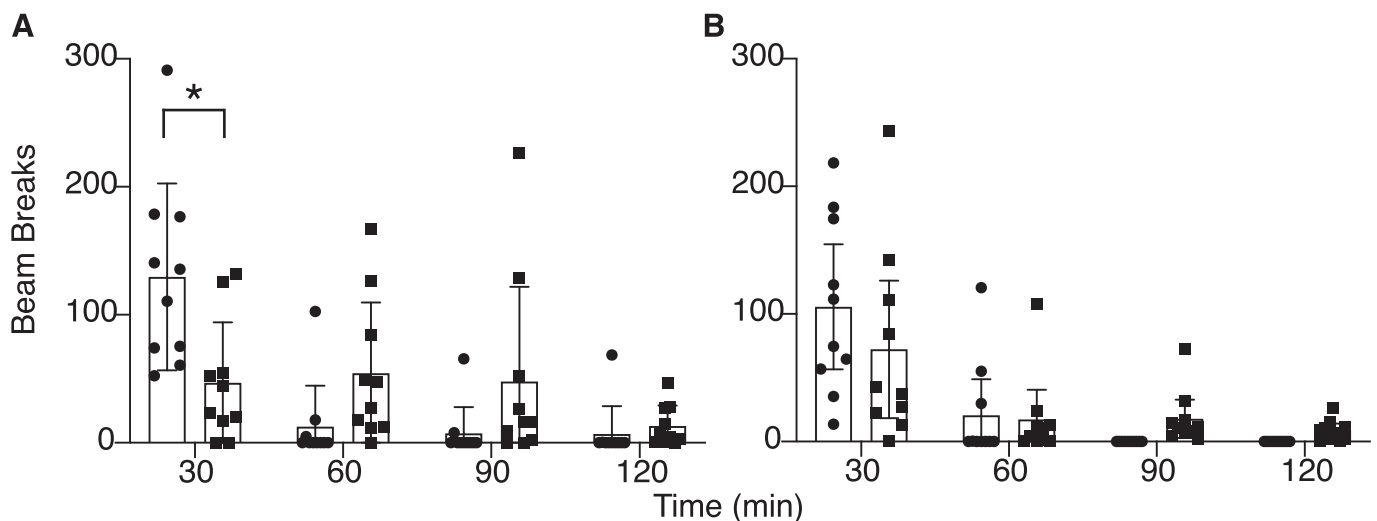


Fig. 6. Time course of the effects of vehicle (○) or Δ^9 -THC (5 mg/kg; ■) administration on motor activity in adult (A) and adolescent (B) mice. Symbols represent mean \pm S.D., $P < 0.05$, $n = 10$ per group, two-way ANOVA.

demonstrated the existence of sex-dependent differences in the biotransformation of Δ^9 -THC into 11-OH-THC in adolescent rats (Wiley and Burston, 2014), and similar dimorphisms are also likely to occur in mice. Indeed, a comparative survey of the PK properties of Δ^9 -THC in male and female adolescent mice is currently underway in our laboratory. Second, cannabis extracts contain hundreds of chemical constituents, which may impact the PK properties of Δ^9 -THC. For instance, cannabidiol may inhibit Δ^9 -THC metabolism via CYP3A11 (Stout and Cimino, 2014), whereas some terpenoids (e.g., borneol) may alter blood-brain barrier permeability (Yin et al., 2017).

In sum, our experiments reveal the existence of substantial differences in the distribution and metabolism of Δ^9 -THC between adolescent and adult male mice—a result with meaningful implications for the interpretation of studies comparing Δ^9 -THC effects in these two age groups. In particular, adolescent animals show higher peak concentrations of Δ^9 -THC in circulation along with more extensive CYP₄₅₀-mediated metabolism and reduced entry of the drug into the brain. The developmental variations in Δ^9 -THC absorption and metabolism across the lifespan clearly deserve further study in both animal models and humans.

Authorship Contributions

Participated in research design: Torrens, Mahler, Das, Piomelli.
Conducted experiments: Torrens, Vozella, Huff, McNeil, Ahmed.
Performed data analysis: Torrens, Vozella, Huff, Ghidini.
Wrote or contributed to the writing of the manuscript: Torrens, Mahler, Huestis, Piomelli.

References

- Agurell S, Halldin M, Lindgren JE, Ohlsson A, Widman M, Gillespie H, and Hollister L (1986) Pharmacokinetics and metabolism of delta 1-tetrahydrocannabinol and other cannabinoids with emphasis on man. *Pharmacol Rev* **38**:21–43.
- Burston JJ, Wiley JL, Craig AA, Selley DE, and Sim-Selley LJ (2010) Regional enhancement of cannabinoid CB₁ receptor desensitization in female adolescent rats following repeated delta-tetrahydrocannabinol exposure. *Br J Pharmacol* **161**:103–112.
- Christensen HD, Freudenthal RI, Gidley JT, Rosenfeld R, Boegli G, Testino L, Brine DR, Pitt CG, and Wall ME (1971) Activity of delta⁸- and delta⁹-tetrahydrocannabinol and related compounds in the mouse. *Science* **172**:165–167.
- Cooper ZD and Haney M (2009) Comparison of subjective, pharmacokinetic, and physiological effects of marijuana smoked as joints and blunts. *Drug Alcohol Depend* **103**:107–113.
- Fanali G, Cao Y, Ascenzi P, Trezza V, Rubino T, Parolaro D, and Fasano M (2011) Binding of δ^9 -tetrahydrocannabinol and diazepam to human serum albumin. *IUBMB Life* **63**:446–451.
- Gabrielsson J and Weiner D (2012) Non-compartmental analysis. *Methods Mol Biol* **929**:377–389.
- Goodall EF, Wang C, Simpson JE, Baker DJ, Drew DR, Heath PR, Saffrey MJ, Romero IA, and Wharton SB (2018) Age-associated changes in the blood-brain barrier: comparative studies in human and mouse. *Neuropathol Appl Neurobiol* **44**:328–340.
- Greene C, Hanley N, and Campbell M (2019) Claudin-5: gatekeeper of neurological function. *Fluids Barriers CNS* **16**:3.
- Gunasekaran N, Long LE, Dawson BL, Hansen GH, Richardson DP, Li KM, Arnold JC, and McGregor IS (2009) Reintoxication: the release of fat-stored delta⁹-tetrahydrocannabinol (THC) into blood is enhanced by food deprivation or ACTH exposure. *Br J Pharmacol* **158**:1330–1337.
- Huestis MA (2007) Human cannabinoid pharmacokinetics. *Chem Biodivers* **4**:1770–1804.
- Huestis MA and Cone EJ (2004) Relationship of Δ^9 -tetrahydrocannabinol concentrations in oral fluid and plasma after controlled administration of smoked cannabis. *J Anal Toxicol* **28**:394–399.
- Huff HC, Maroutsos D, and Das A (2019) Lipid composition and macromolecular crowding effects on CYP2J2-mediated drug metabolism in nanodiscs. *Protein Sci* **28**:928–940.
- Johansson E, Norén K, Sjövall J, and Halldin MM (1989) Determination of delta 1-tetrahydrocannabinol in human fat biopsies from marijuana users by gas chromatography-mass spectrometry. *Biomed Chromatogr* **3**:35–38.
- Johnston LD, Miech RA, O'Malley PM, Bachman JG, Schulenberg JE, and Patrick ME (2019) Monitoring the future national survey results on drug use, 1975–2018: overview, key findings on adolescent drug use.
- Kalant H (2015) Cannabis control policy: no rational basis yet for legalization. *Clin Pharmacol Ther* **97**:538–540.
- Kreuz DS and Axelrod J (1973) Delta-9-tetrahydrocannabinol: localization in body fat. *Science* **179**:391–393.
- Leishman E, Murphy M, Mackie K, and Bradshaw HB (2018) Δ^9 -Tetrahydrocannabinol changes the brain lipidome and transcriptome differentially in the adolescent and the adult. *Biochim Biophys Acta Mol Cell Biol Lipids* **1863**:479–492.
- Lubman DI, Cheetham A, and Yücel M (2015) Cannabis and adolescent brain development. *Pharmacol Ther* **148**:1–16.
- Lucas CJ, Galettis P, and Schneider J (2018) The pharmacokinetics and the pharmacodynamics of cannabinoids. *Br J Clin Pharmacol* **84**:2477–2482.
- McDougle DR, Kambalal A, Meling DD, and Das A (2014) Endocannabinoids anandamide and 2-arachidonoylglycerol are substrates for human CYP2J2 epoxidase. *J Pharmacol Exp Ther* **351**:616–627.
- Nitta T, Hata M, Gotoh S, Seo Y, Sasaki H, Hashimoto N, Furuse M, and Tsukita S (2003) Size-selective loosening of the blood-brain barrier in claudin-5-deficient mice. *J Cell Biol* **161**:653–660.
- Pertwee RG (2008) The diverse CB₁ and CB₂ receptor pharmacology of three plant cannabinoids: delta⁹-tetrahydrocannabinol, cannabidiol and delta⁹-tetrahydrocannabinol. *Br J Pharmacol* **153**:199–215.
- Pfaffl MW, Tichopad A, Prgomet C, and Neuvians TP (2004) Determination of stable housekeeping genes, differentially regulated target genes and sample integrity: BestKeeper—Excel-based tool using pair-wise correlations. *Biotechnol Lett* **26**:509–515.
- Piomelli D (2015) Neurobiology of marijuana, in *The American Psychiatric Publishing Textbook of Substance Abuse Treatment*, 5th ed (Galanter M, Kleber HD, and Brady K 335–350, American Psychiatric Publishing, Arlington, VA).
- Rawitch AB, Rohrer R, and Vardaris RM (1979) delta-9-Tetrahydrocannabinol uptake by adipose tissue: preferential accumulation in gonadal fat organs. *Gen Pharmacol* **10**:525–529.
- Rubino T and Parolaro D (2016) The impact of exposure to cannabinoids in adolescence: insights from animal models. *Biol Psychiatry* **79**:578–585.
- Sadler NC, Nandhikonda P, Webb-Robertson BJ, Ansong C, Anderson LN, Smith JN, Corley RA, and Wright AT (2016) Hepatic cytochrome P450 activity, abundance, and expression throughout human development. *Drug Metab Dispos* **44**:984–991.
- Schweinsburg AD, Brown SA, and Tapert SF (2008) The influence of marijuana use on neurocognitive functioning in adolescents. *Curr Drug Abuse Rev* **1**:99–111.
- Sethi PK, White CA, Cummings BS, Hines RN, Muralidhara S, and Bruckner JV (2016) Ontogeny of plasma proteins, albumin and binding of diazepam, cyclosporine, and deltamethrin. *Pediatr Res* **79**:409–415.
- Spear LP (2000) The adolescent brain and age-related behavioral manifestations. *Neurosci Biobehav Rev* **24**:417–463.
- Spiro AS, Wong A, Boucher AA, and Arnold JC (2012) Enhanced brain disposition and effects of Δ^9 -tetrahydrocannabinol in P-glycoprotein and breast cancer resistance protein knockout mice. *PLoS One* **7**:e35937.
- Steinberg L (2005) Cognitive and affective development in adolescence. *Trends Cogn Sci* **9**:69–74.
- Stout SM and Cimino NM (2014) Exogenous cannabinoids as substrates, inhibitors, and inducers of human drug metabolizing enzymes: a systematic review. *Drug Metab Rev* **46**:86–95.
- Vozella V, Zibardi C, Ahmed F, and Piomelli D (2019) Fast and sensitive quantification of Δ^9 -tetrahydrocannabinol and its main oxidative metabolites by liquid chromatography/tandem mass spectrometry. *Cannabis Cannabinoid Res* **4**:110–123.
- Wahlqvist M, Nilsson IM, Sandberg F, and Agurell S (1970) Binding of delta-1-tetrahydrocannabinol to human plasma proteins. *Biochem Pharmacol* **19**:2579–2584.
- Watanabe K, Narimatsu S, Matsunaga T, Yamamoto I, and Yoshimura H (1993) A cytochrome P450 isozyme having aldehyde oxygenase activity plays a major role in metabolizing cannabinoids by mouse hepatic microsomes. *Biochem Pharmacol* **46**:405–411.
- Watanabe K, Yamamoto I, Oguri K, and Yoshimura H (1980) Comparison in mice of pharmacological effects of delta 8-tetrahydrocannabinol and its metabolites oxidized at 11-position. *Eur J Pharmacol* **63**:1–6.
- Wiley JL and Burston JJ (2014) Sex differences in Δ^9 -tetrahydrocannabinol metabolism and in vivo pharmacology following acute and repeated dosing in adolescent rats. *Neurosci Lett* **576**:51–55.
- Wong A, Montebello ME, Norberg MM, Rooney K, Lintzeris N, Bruno R, Booth J, Arnold JC, and McGregor IS (2013) Exercise increases plasma THC concentrations in regular cannabis users. *Drug Alcohol Depend* **133**:763–767.
- Yin Y, Cao L, Ge H, Duanmu W, Tan L, Yuan J, Tunan C, Li F, Hu R, Gao F, et al. (2017) L-Borneol induces transient opening of the blood-brain barrier and enhances the therapeutic effect of cisplatin. *Neuroreport* **28**:506–513.

Address correspondence to: Daniele Piomelli, Anatomy and Neurobiology, Gillespie Neuroscience Research Facility, 837 Health Sciences Rd., Room 3101, Irvine, CA 92697. E-mail: piomelli@hs.uci.edu